

# Multiscale assessment on the quality of metal powder feedstocks for additive manufacturing

By Xinwei Wang, Karol Putyera, Boris Albouy, Pat McKeown, Jim Gibson, and Sasha Rodnyansky

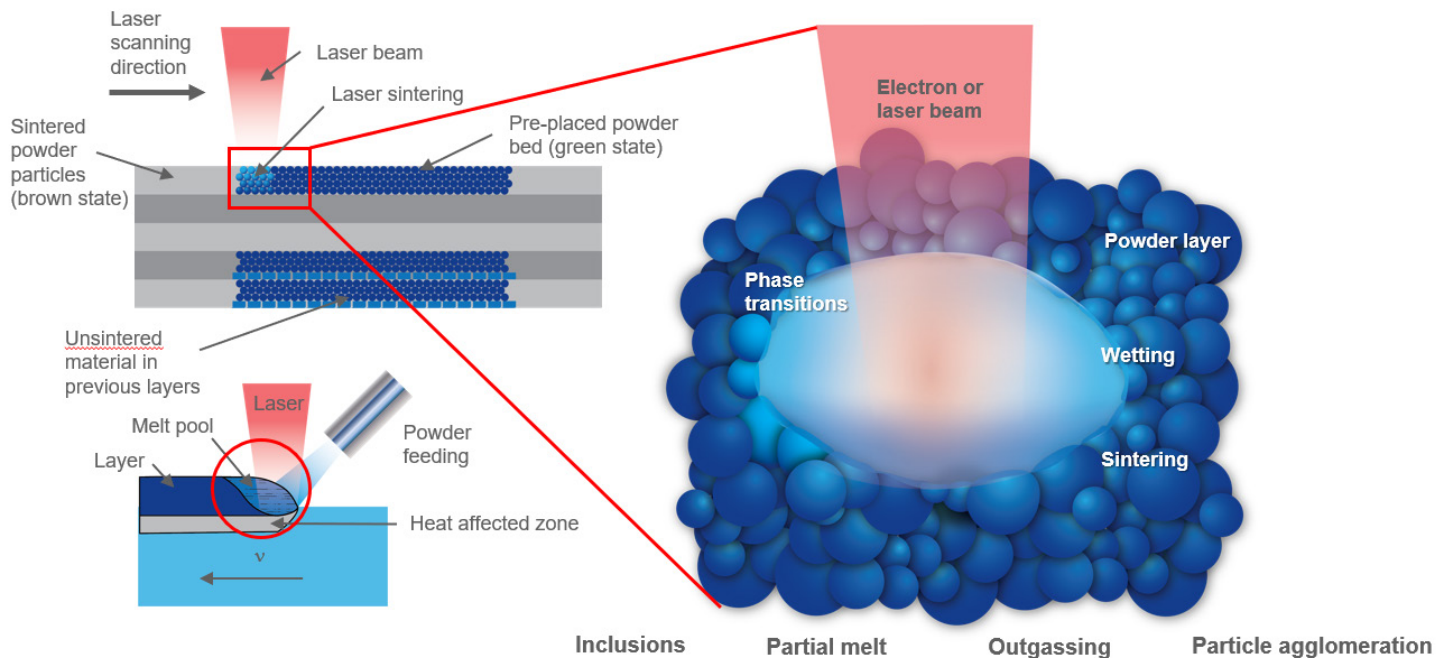
## INTRODUCTION

Additive manufacturing (AM) is attractive for producing parts with access to unprecedented geometry/configuration complexity, material composition gradient control, and lightweight structure design not attainable by traditional processes. However, the long-term success of this rapidly developing technology hinges, to a large degree, on the ability to produce functional parts and components reliably. Controlling defects is of primary importance to attain AM metal parts with mechanical strength and fatigue life approaching their forged counterparts. Defects in AM parts fall into two main categories: porosity and crack. These can be incurred by various mechanisms: lack of fusion, keyhole collapse, gas porosity, balling, solidification cracking, solid-state cracking, and surface-connected porosity. Defects can also result from entrapment of impurities.<sup>1</sup> Defects arise from the interplay between feedstock and AM beam energy, which involves complex, transient thermophysical and chemical processes (Scheme 1). As such, defects can be feedstock-, equipment-, and processes-related.<sup>2</sup> Consequently, defect reduction starts with the quality

control of feedstocks.

Two mainstream AM technologies, i.e., laser powder bed fusion (PBF) and blown powder direct energy deposition (DED), use spherical powder feedstocks with the desired compositions and particle sizes, typically in the range of 10 to 50 microns. In this kind of matter in particulate form, the population of surface and sub-surface atoms represent four to five orders larger ratio as compared to bulk materials. While bulk chemistry still lays the foundation for ultimate mechanical properties, the surface chemistry of micro sized powders is becoming equally important, if not greater, for the quality of finished AM parts. Driven by the increased surface free energy (i.e., thermodynamic favorable) and the decrease in diffusion length (i.e., kinetic favorable), the particle-to-particle uniformity of AM metal powder is inherently susceptible to local events such as surface contamination, agglomeration, and composition variation, during powder manufacturing, packaging, storage, use and reuse.<sup>3</sup>

As defects arise in multiple length scales, it calls for analytical solutions with multi-length scale sampling capability. Numerous institutes have engaged in standardizing testing methods for AM powder feedstocks<sup>13</sup>. This white paper is not intended to repeat



Scheme 1. Illustrative PBF and DED AM processes, and the powder/beam interaction in the melt pool

# Multiscale assessment on the quality of metal powder feedstocks for additive manufacturing

these efforts; rather, we focus on selecting a few techniques, each with certain length-scale sampling capability, for identifying and quantitatively assessing the quality of AM metal powder feedstocks, e.g. Ti6Al4V AM powder (Figure 1). Combination of these techniques (Scheme 2) enable multiscale sampling and uniformity assessment of AM metal powder feedstock:

- from single particle to  $10^{7-8}$  particles
- from a few surface atomic layers (nm-depth) to bulk (10s- $\mu\text{m}$  depth)
- from elemental information to valence chemistries, and
- from %-level composition elements to sub-ppm trace impurities

## 2. SURFACE CHEMISTRY CHARACTERIZATION OF AM METAL POWDER FEEDSTOCK

### 2.1 Volume fraction of the native oxide film on AM metal powder

“God made the bulk; the surface was invented by the devil – Wolfgang Pauli”. AM metal powders carry  $10^{4-5}$  - fold more surface and sub-surface atom population than typical bulk materials. These surface and sub-surface atoms are prone to reacting with residual oxygen, even at the highest practical vacuum that could be attained. For common reactive metals, such as Al and Ti, only at extremely low oxygen partial pressures, e.g.,  $10^{-16}$  atm for liquid Ti,<sup>4</sup> can oxidation be avoided. Thus, AM metal or alloy powders containing reactive metals, such as Al, Ti, Cr, Zr, Nb, and Ta, are known to develop conformable, continuous, native oxide thin films. The thickness of these films can vary from a few to tens of nanometers, depending on manufacturing processes, storage conditions and thermal history.

The volume fraction of surface oxide can be estimated for particles

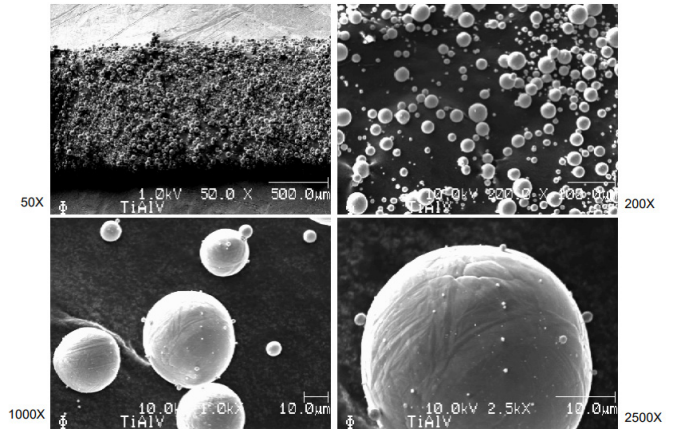
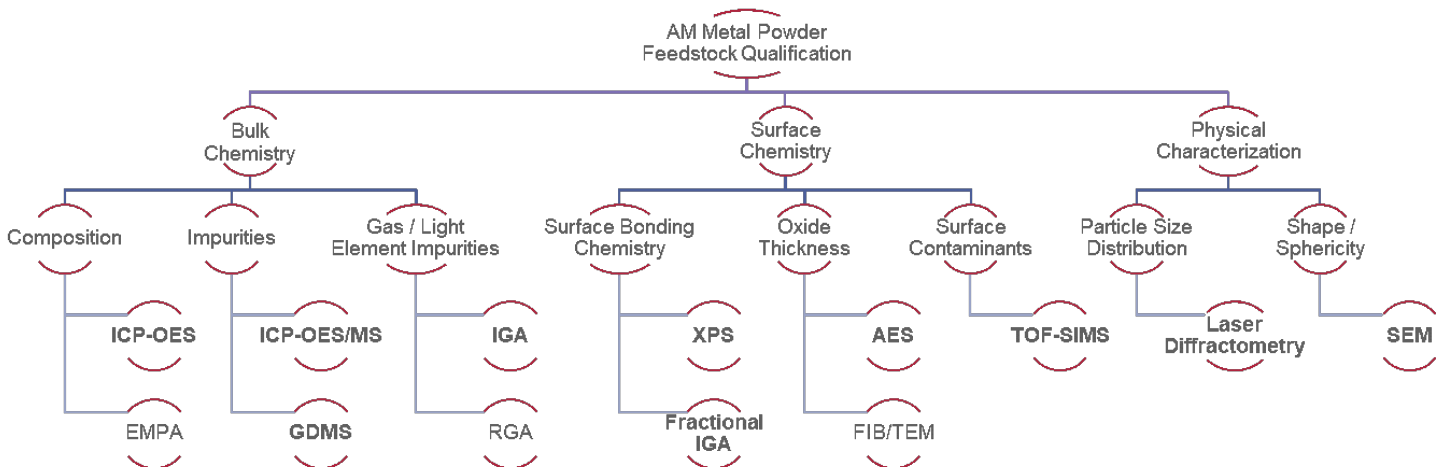


**Figure 1. Secondary electron images of Ti6Al4V powder at 50x, 200x, 1000x, and 2500x magnifications**

with perfect sphericity, if the oxide film is uniformly covering the particle, using the following equation:

$$\text{Oxide Vol\%} = [1 - (1 - 2t/d)^3] \times 100\% \\ \approx \frac{6t}{d} \times 100\% \text{ when } \frac{t}{d} \ll 0$$

where  $d$  – particle diameter, and  $t$  – oxide film thickness. It shows that the oxide volume fraction increases linearly with oxide film thickness, but inverse proportionally with the particle size. Figure 2 presents a few slices of correlation of the estimated oxide volume with oxide film thickness for spheric particles in 5 – 50  $\mu\text{m}$  diameter range. For a particle of 10  $\mu\text{m}$  in diameter, the volume fraction of the surface oxide can be up to 1.2 v% for powders developed an oxide film thickness of 20 nm, which is common for Ti6Al4V AM powders produced by plasma atomization.



**Scheme 2. Suggested characterization techniques for qualifications of AM metal powder feedstock. Only those in bold are demonstrated in this paper.**

# Multiscale assessment on the quality of metal powder feedstocks for additive manufacturing

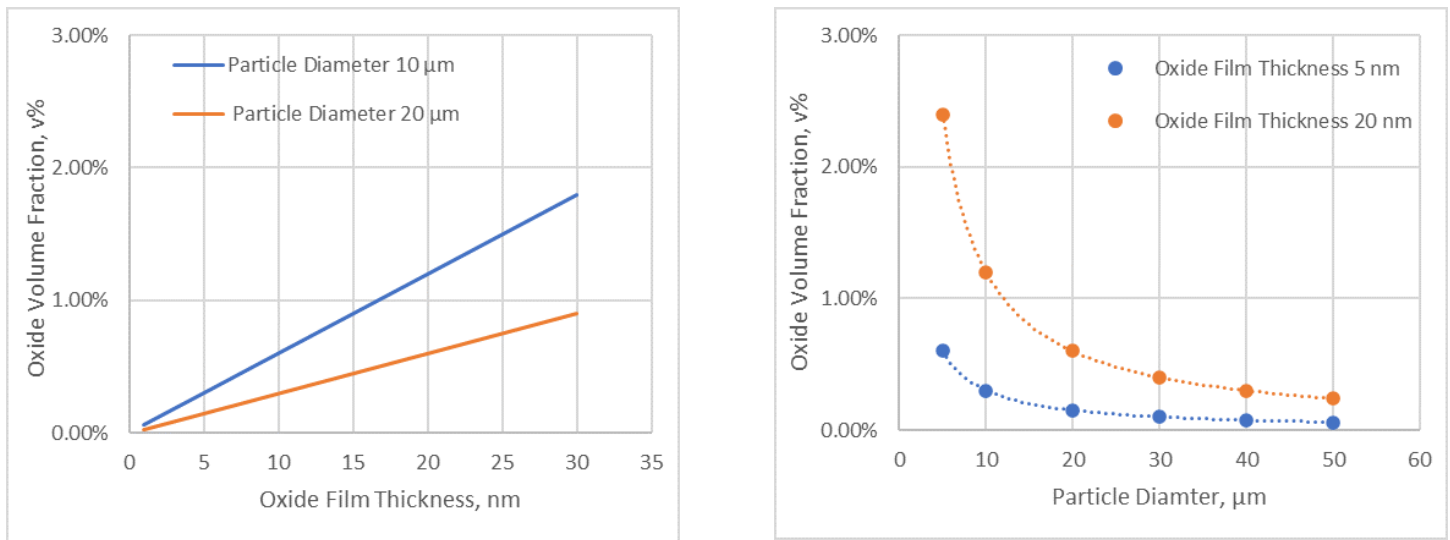


Figure 2. Correlation of estimated oxide volume fraction (v%) with oxide film thickness and particle diameter for spherical Ti6Al4V AM powders

This oxide film is rich in chemistry and physics, e.g., surface – OH, oxygen vacancies, cation vacancies, amorphous oxides, and dramatic impurity enrichment driven by segregation. All alter, and often, increase surface polarity and binding energy for moisture and organic contaminant physisorption. They represent a significant source for defect formation. Studying these details

requires techniques with nm-spatial resolution for elemental and chemical information.

## 2.2 Determination of oxide thickness and depth profiling of single AM metal particle by Auger Electron Spectroscopy (AES)

The oxide film developed on metal powder can be problematic for AM processing, causing partial melting or lack of fusion, balling,

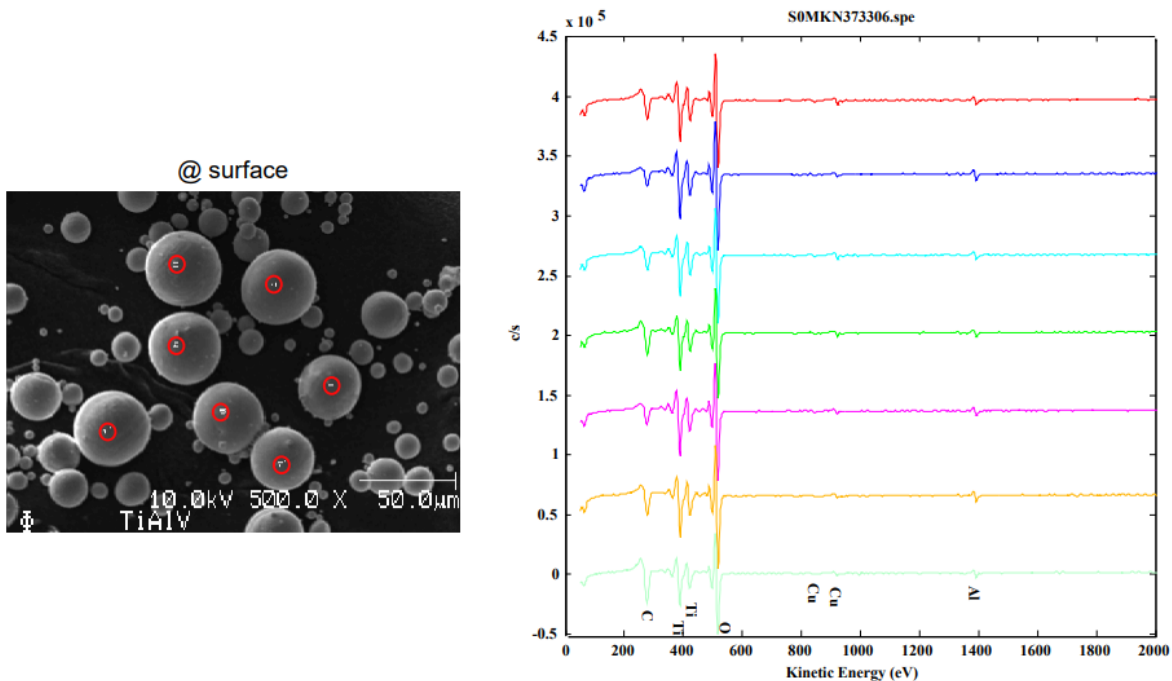


Figure 3. Secondary Electron Image (SEI) and Auger surface survey spectra on multiple AM Ti6Al4V particles (Sigma Aldrich). Probed particles are 20-30 μm in diameter. One area was analyzed per particle (circled in red). Surface Cu and C contamination was identified. Ti, O and Al are present within the top 5 nm as composition elements, but V is absent

# Multiscale assessment on the quality of metal powder feedstocks for additive manufacturing

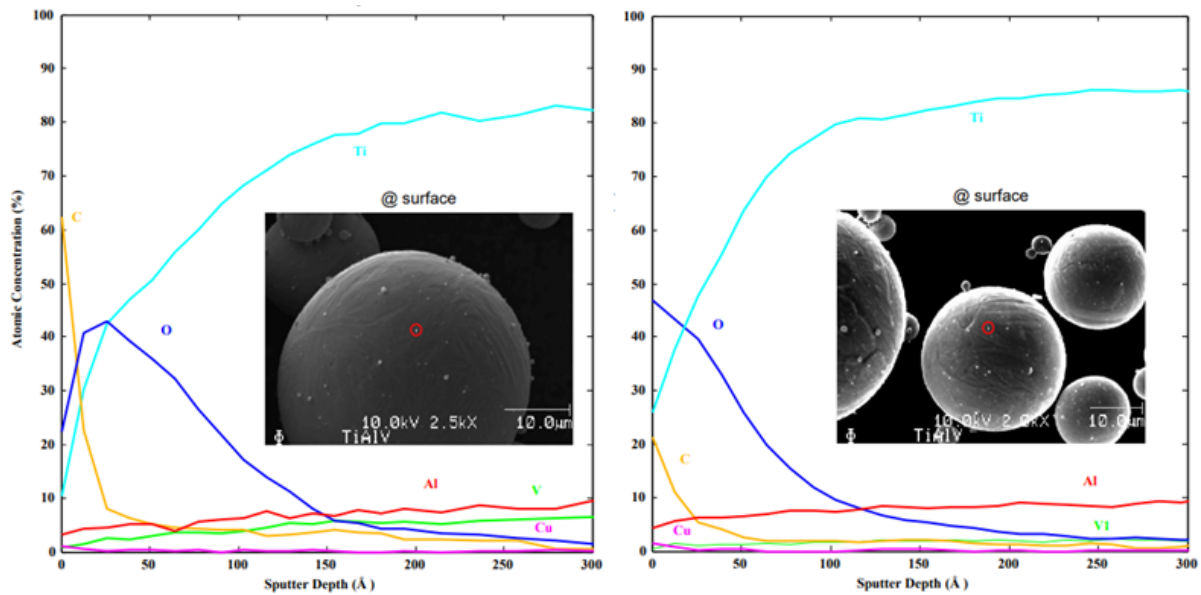


Figure 4. Auger depth profiling on two AM Ti6Al4V particles (Sigma Aldrich), showing surface Cu and C contamination at the top 5 nm. Inserted are the SEI image and sampling locations on the particle. The two particles show significant difference in oxygen, with determined oxide thickness 8 nm (a) and 6 nm (b), respectively.

poor wetting, and evaporation loss of key alloying elements, e.g., Cr and Mo as volatile oxides when they are enriched in the surface. AES is a surface-sensitive analytical technique that utilizes a high-energy electron beam as an excitation source to probe the elemental composition of top 3 - 25 nm. With a small electron beam diameter, AES can accurately position and focus the electron beam on a small area (< 25 nm) of a particle. As such, AES is well suited to measure oxide thickness and depth profiles of compositional elements above sub-% level on individual AM metal powder particle.

Figure 3 shows the secondary electron images and AES survey data of multiple AM TiAl4V powders. Particles probed are 20-30  $\mu\text{m}$  in diameter, with one area analyzed per particle. Surface %-level Cu and C impurities were detected in the top 5 nm. Carbon is the source of carbide inclusions, while Cu can induce contamination cracking.<sup>5</sup>

Figure 4 presents the depth profiling of two Ti6Al4V particles in nm-resolution, showing difference in oxygen, carbon, and Cu profiles. Vanadium was absent in the top few nanometers, indicating that the top oxide layers are comprised of Ti and Al oxides only. Two particles also developed different oxide thickness, 6 and 8 nm, respectively. These results demonstrate that AES can provide atomic level details relevant to deflection formation in AM parts, including surface contamination, oxide composition, element concentration gradient, and oxide thickness on single particle, at nm-spatial resolution. By surveying multiple particles, it also enables particle-to-particle consistency evaluation.

## 2.3 Surface contaminants and elemental mapping of multiple AM powder particles by TOF-SIMS

Time-of-Flight Secondary Ion Mass Spectrometry (TOF-SIMS) is another surface analytical technique. It is a great technique for analyzing trace and thin organic on solid surfaces. It will also detect elemental species to trace levels. Features down to a few microns in size and one nanometer thick can be analyzed.

The technique uses an ion beam and mass spectrometer to analyze the sample. An ion beam is pulsed to the sample surface causing a pulse of sample ions to be ejected. These secondary ions are accelerated in an electric field and the flight times to a detector are measured. Ion kinetic energies being equal means lighter ions will have higher velocities and will arrive at the detector first, such as hydrogen, and heavier ions will get there later such as organic molecules. Measuring flight time very accurately allows for determination of mass and molecular formula. Generated are high resolution mass spectra, images, and depth profiles.

Figure 5 presents the TOF-SIMS data of Ti6Al4V, NiTi and Al powders (Sigma Aldrich) in negative ion mode. Based on the mass fragmentation pattern, the surface contamination nature can be identified, for example,

- Ti6Al4V surface had phthalate contamination, OH and corrosive Cl, Br, Phosphate, S, and nitrogen oxide species
- NiTi surface had detergent contamination
- Al surface was decorated by various Al-OH, Al-O chemistries

Figure 6(a) presents the TOF-SIMS ion images of AM Ti6Al4V powder surface. Surface compositions were evaluated on particles

# Multiscale assessment on the quality of metal powder feedstocks for additive manufacturing

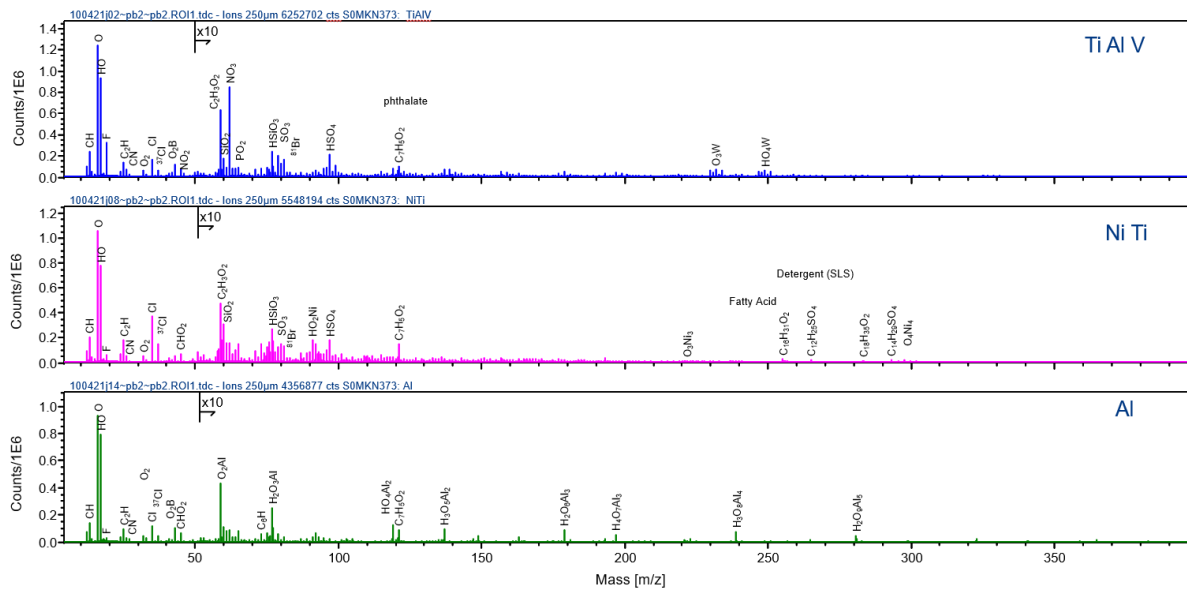


Figure 5. TOF-SIMS spectra of Ti6Al4V, NiTi and Al powders in negative ion mode.

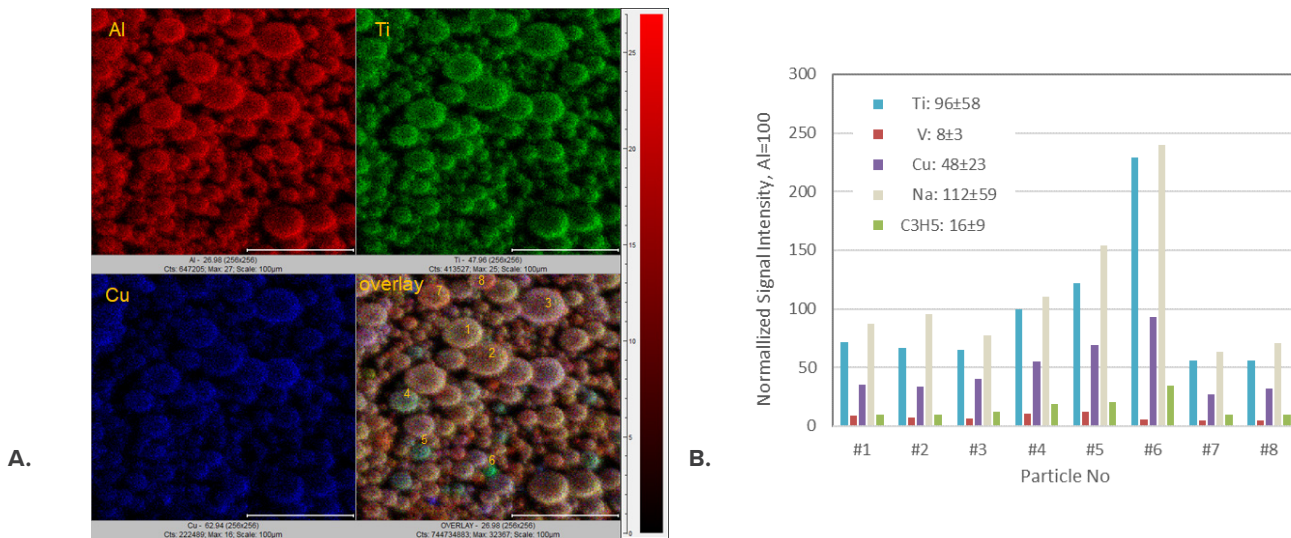


Figure 6. (a) TOF-SIMS ion image of AM Ti6Al4V powders; (b) Surface concentration of Ti, V, Cu, and Na of particles “1” through “8”, normalized to Al signal (Al = 100). Information depth is approximately 1 nm. Particle-to-particle variation are presented in the legend, as average  $\pm$  SD over eight particles.

labelled “1” through “8”. The relative concentration is normalized to Al signal (Al = 100), from an estimated sampling depth of 1 nm. Figure 6(b) illustrates several species of high ion signal intensity, including Ti, V, Cu, Na, and characteristic hydrocarbon fragment  $-C_3H_5$ . The mean value and standard deviation were evaluated over eight particles, with Ti/Al  $96 \pm 58$ , V/Al  $8 \pm 3$ , Cu/Al  $48 \pm 23$ , Na/Al  $112 \pm 59$ , and  $C_3H_5$ /Al  $16 \pm 9$ . The large standard deviation indicated that particle-to-particle chemistry variation is significant, whether for composition elements (Ti and V), elemental contaminants (Cu and Na), or hydrocarbon contaminant ( $-C_3H_5$ ).

These surface characteristics could introduce defects in finished

AM parts by various mechanisms, such as poor interlayer fusion, gas porosity ( $H_2O$  and  $H_2$ ), carbide inclusions, corrosion-susceptible species (Cl, Br, S, P, NOx). Surface residual moisture and -OH groups also increase the susceptibility to humidity and therefore affect the flowability of AM powder feedstock.

### 3.3 Surface bonding chemistry of AM powder by XPS at $10^{-7-8}$ particle scale

X-Ray Photoelectron Spectroscopy (XPS Spectroscopy) uses monochromatic X-rays to irradiate a sample. The binding energies of emitted photoelectrons are characteristic of the elements present on the surface and their valence states. Since only



# Multiscale assessment on the quality of metal powder feedstocks for additive manufacturing

alloy with a wide solidification temperature range may also exhibit a less coherent dendritic structure during solidification, thus preventing liquid from backfilling to shrinkage cracks.<sup>5</sup> (2) change in density, heat capacity and thermal conductivity can lead to uneven beam energy absorption, triggering various AM process - related porosity mechanisms, e.g., lack of fusion, keyhole collapse, sputtering, etc. Presence of light elements, such as C, H, O and N, can lead to gas porosity, and various precipitates and inclusions. Some impurities, even at trace levels, can have tremendous impact, often detrimental to reliability: (1) S and P are known to cause solidification cracking for ferrous and nickel alloys, as are Mg and Cu impurities to aluminum alloys.<sup>5</sup>; (2) Low melting point impurities (including Zn, Ga, Cd, In, Sn, Sb, Pb, and Bi), and S, Cl, As, Se, and Te, are responsible for drop in rupture toughness and corrosion resistance; and (3) leachable heavy metals from AM medical devices can generate toxicity concerns, as specified in USP < 232 > and ICH Q3D, including As, Cd, Hg, and Pb.

Techniques with large sampling sizes are critical to provide complete and representative assessments of feedstock compositions. However, suitable analytical protocols must be developed and qualified to provide sensitive, precise, accurate, robust, and full survey assays. As an example, Eurofins EAG Laboratories participated in an interlaboratory analysis program organized by LGC Standards Ltd. for such development of methods. Table 2 shows our results from that interlaboratory study for IARM Ti64P-18 Additive Manufacturing Powder. We used Inductively Coupled Plasma - Optical Emission and Mass Spectrometry (ICP-OES/MS) methods and Inert Gas Fusion and Combustion techniques (IGA) for this study. These techniques require sampling amounts in the range of 0.1 g to 1 g (equivalent to about 10<sup>7-8</sup> particles) for determining mass fractions of analytes listed in Table 1. The high accuracy and precision demonstrated here confirms that optimized ICP-OES/MS and IGA test methods can readily capture within lot, and lot-to-lot chemistry variations in this kind of AM powder feedstocks.

**Table 2. Test Results on LGC - IARM Ti64P-18 Additive Manufacturing Powder**

Elements	EAG Measured		Certified
	Technique	Mean ± SD (n=4), %mass	Mean ± U <sub>CRM</sub> <sup>*</sup> , %mass
Ti	ICP-OES	88.9 ± 0.01	(88.7)
Al	ICP-OES	6.64 ± 0.01	6.47 ± 0.09
Fe	ICP-OES	0.209 ± 0.001	0.216 ± 0.005
V	ICP-OES	4.30 ± 0.01	4.24 ± 0.05

C	IGA (Combustion – IR)	0.048 ± 0.001	0.051 ± 0.004
O	IGA (Inert Gas Fusion – IR)	0.17 ± 0.004	0.15 ± 0.02
S	IGA (Combustion – IR)	0.0013 ± 0.0005	0.0014 ± 0.0006
Mn	ICP-MS	0.011 ± 0.0004	0.011 ± 0.0002
P	ICP-MS	0.0010 ± 0.0004	(0.0010)
Cu	ICP-MS	0.0062 ± 0.0004	(< 0.0050)
* uncertainty associated with the measurement was estimated with coverage factor $k = 2$ at approximately 95% confidence level.			

Aside from solution based ICP-OES/MS, solid sampling high mass resolution glow discharge mass spectrometry (GDMS) is another suitable analytical technique for chemical analysis of AM powder feedstocks. The main advantages of GDMS as compared to other techniques are: (1) direct sampling, thus avoiding tedious sample preparations; (2) full survey elemental analysis capability, allowing determination of up to 72 elements in a single test, including all stable isotopes [6]; and (3) superior sensitivity at sub-µg/g levels, even for such critical elements as P, S, Cl, As, Se, Bi, among others.

Typically, GDMS measurements are evaluated based on atomizing several mm<sup>3</sup> of volume fractions (8 - 10 mm in diameter x tens of µm in depth), which are equivalent to tens of mg sampling amounts, or about 10<sup>5</sup> particles per test. Hence, GDMS is well suited as a production control tool to monitor trace and ultra-trace level fluctuation of all detrimental impurities not only in feedstocks but also in final metal components that are intended to operate under harsh / extreme working environments. As an example, the smallest concentration (or amount) of analytes that are typically reported from GDMS measurements for selected impurities in Ti6Al4V AM powder sample are summarized in Table 3. Note that in titanium-based samples either an alternative discharge gas (Krypton instead or Argon) needs to be used or the glow-discharge source needs to be operated in pulsed fast-flow modes to measure mass fractions of certain elements with low specification limits, such as yttrium with max 50 µg/g per ASTM F3007.

Therefore, it is recommended that for AM metal parts graded for critical applications, such as Inconel® 718 and Haynes® 282 superalloy, their powder feedstock be evaluated with advanced GDMS methods for key impurities listed in Table 3.

# Multiscale assessment on the quality of metal powder feedstocks for additive manufacturing

**Table 3. GDMS analytical characteristics for selected impurities in Ti6Al4V AM powder**

GDMS Analytical Capability		Impurity Role in Ti6Al4V				
Elemental Capability (Partial)	Reporting Limit, $\mu\text{g/g}$	Solidification Cracking	Mechanical Strength	Corrosion Resistance	Fatigue Lifetime	Toxicity
B	0.01	—	↑	—	—	—
Si	0.1	—	↑	—	—	—
S	0.01	↑	↓	↓	↓	—
P	0.01	↑	↓	↓	↓	—
Cl	0.01	—	↓	↓	↓	—
As	0.5	—	↓	↓	↓	↑
Se	1	↑	↓	↓	↓	↑
Te	0.1	↑	↓	↓	↓	—
Cr	0.1	—	—	—	—	↑
Fe	0.1	—	—	—	—	—
Cu	0.1	↑	↓	↓	↓	↑
Zn	0.5	—	↓	↓	↓	—
Y	200*/15**	—	—	—	—	—
Mo	0.5	—	↑	↑	↑	↑
Cd	0.1	—	↓	↓	↓	↑
In	0.01	—	↓	↓	↓	—
Sn	0.1	—	↓	↓	↓	—
Sb	0.5	—	↓	↓	↓	—
Hg	0.1	—	↓	↓	↓	↑
Pb	0.05	—	↓	↓	↓	↑
Bi	0.05	—	↓	↓	↓	—

\* Y reporting limit using Ar as discharge gas; \*\* the same by fast-flow test method. ↓ decrease; ↑ increase; — no change or unknown

## 3.2 Fractional gas analysis of O, N and H at $10^{7-8}$ – particle scale

Taking advantage of the temperature-programming capability of specific inert gas fusion (IGA) instrument models, Eurofins EAG Laboratories also developed fractional gas analysis protocols for quantitatively assessing the O, N and H chemistries in powders, such as surface and interface oxygen, oxide precipitates, interstitial oxygen, surface -OH or physisorbed moisture, from % levels to  $\mu\text{g/g}$  levels.<sup>7</sup> The sampling amounts in the fractional analysis methods are the same as in standard IGA protocols, which are between 0.1 and 1.0 g per test. These amounts are equivalent to about  $10^{7-8}$  particles per test.

Figure 9(a) illustrates the principles of the fractional gas analysis method. Figure 9(b) shows the oxygen releasing profile of Ti6Al4V AM powder acquired by fractional oxygen analysis method. In this example two distinct oxygen releasing peaks are observed, indicating there are at least two types of oxygen containing groups / species present in this specific example. Previously, AES data have revealed that at least a significant portion of oxygen in AM Ti6Al4V powder is present in the form of surface oxide film. However, as a surface technique, AES is limited to provide surface information. On the other hand, fractional O analysis, as an inert gas fusion technique, detects oxygen based on the carboreduction activity of oxygen in the sample. Surface oxygen is more reactive therefore will be released even at a temperature below fusion. This is not the case for interstitial oxygen; the latter will diffuse out the sample only in the molten state. Therefore, fractional O analysis provides a quantitative means to speciate surface and interstitial oxygen in AM powders, as demonstrated in Figure 9(b).

Notice that the ramp mode yielded about 200  $\mu\text{g/g}$  O and 20  $\mu\text{g/g}$  H lower values than the total O and H determined by the flash mode (Table 4). This difference, with mass ratio O/H ~ 10/1, is attributed to moisture and surface residual -OH groups in Ti6Al4V powder,

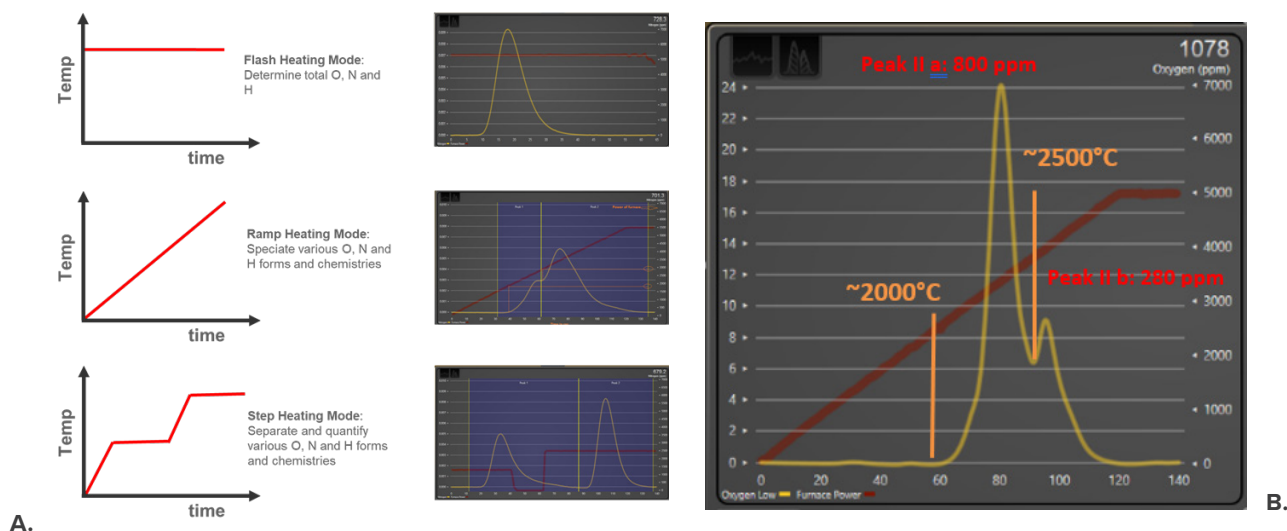


**Figure 9. (a) Fractional IGA O, N and H analysis method development protocol, with N as example; and (b) oxygen releasing profile of Ti6Al4V AM powder acquired by fractional IGA technique, with two distinct oxygen releasing peaks observed.**

# Multiscale assessment on the quality of metal powder feedstocks for additive manufacturing

which are not detected in fractional analysis mode. Previously, TOF-SIMS analysis has identified moisture and -OH groups on Ti6Al4V powder surface. Thermal Desorption Spectroscopy (TDS) can provide more detailed moisture desorption behavior. However, quantification is challenging.<sup>[8]</sup> Herein, fractional gas analysis methods not only enable speciating various O, N and H bonding chemistries, but also provide a quantitative means to assess sub-% to µg/g level moisture and surface -OH groups in gram-level sampling. This information could be key for gas porosity control (such as H<sub>2</sub>O, H<sub>2</sub>), as well as for powder agglomeration and flowability control.

**Table 4. Fractional O and H analysis of Ti6Al4V AM powder**

Analysis Mode	O(n=3), µg/g	H(n=3), µg/g	Remark
Flash Mode	1340 ± 70	30 ± 1	ASTM E1409 method
Ramp Mode	1140 ± 70	10 ± 3	EAG fractional analysis protocol
Moisture/ Residual surface -OH (by Difference)	200	20	In consistent with primary loss of H <sub>2</sub> O based on O/H ratio 10/1 (mass/mass)

## SUMMARY

Satisfactory grade metal powders for AM should possess the following characteristics: high chemical purity and uniformity in allotropic form (no density changes), thermal conductivity, solubility of all critical elements, and spherical shape with desired particle size distributions. In this white paper, we identified and quantitatively assessed the chemistry of AM feedstock that is fundamental to the above requirement using Eurofins EAG Laboratories's various bulk and surface characterization tools. Surface techniques provide fine structural details with atomic and molecular information, at nm – spatial resolution, from single particle to multiple particles; and bulk techniques provide a macro-scale, quantitative assessment of composition consistency and purity level. Table 5 provides a summary of the technique features, sampling length scale, and relevant analytical information.

## ACKNOWLEDGEMENT

Special thanks to Christina Pompo, Susan Dunn, Kevin Lucak, Keith Stanton, Sam Murthy and Tina Heetderks for performing ICP-OES, ICP-MS, IGA testing and coordinating the analyses, and Dr. Rajiv Soman for his scientific input.

# Multiscale assessment on the quality of metal powder feedstocks for additive manufacturing

**Table 5 Multiscale assessment of AM metal powder feedstocks – techniques, sampling scale and analytical information**

Technique		Sampling Scale	Analytical Information
Macro-scale Bulk Analysis	ICP-OES	<ul style="list-style-type: none"> <li>• 0.5 – 1.0 g</li> <li>• <math>10^6</math> – <math>10^7</math> particles</li> </ul>	<ul style="list-style-type: none"> <li>• accurate alloy composition analysis from % to sub%</li> <li>• measurement uncertainty less than 1%rel in high performance mode</li> </ul>
	IGA	<ul style="list-style-type: none"> <li>• 0.1 – 1.0 g</li> <li>• <math>10^6</math> – <math>10^7</math> particles</li> </ul>	<ul style="list-style-type: none"> <li>• accurate determination of trace gas-forming element content C, H, O, N and S down to ppm level</li> </ul>
	ICP-MS	<ul style="list-style-type: none"> <li>• 0.1 – 1.0 g</li> <li>• <math>10^6</math> – <math>10^7</math> particles</li> </ul>	<ul style="list-style-type: none"> <li>• accurate trace metal/metalloid impurity analysis with detection limits generally in ppm level</li> <li>• excluding halogen</li> </ul>
	GDMS	<ul style="list-style-type: none"> <li>• 10s mg</li> <li>• <math>10^5</math> particles</li> </ul>	<ul style="list-style-type: none"> <li>• Survey trace metal/metalloid/nonmetal impurity analysis with detection limits generally at sub-ppm level</li> <li>• including S and halogen</li> </ul>
Macro- and Micro-scale Surface Analysis	TOF-SIMS	<ul style="list-style-type: none"> <li>• Analytical area: 250 <math>\mu</math>m x 250 <math>\mu</math>m</li> <li>• 10s-100s particles</li> </ul>	<ul style="list-style-type: none"> <li>• information depth: a few surface atomic layers</li> <li>• Survey identification of molecular contaminants physisorped on the surface, particularly of organic nature</li> <li>• surface composition uniformity from particle to particle</li> </ul>
	AES	<ul style="list-style-type: none"> <li>• Analytical area: &lt; 25 nm</li> <li>• Single particle</li> <li>• Sampling depth: 1-10 nm</li> </ul>	<ul style="list-style-type: none"> <li>• Information depth 5 nm or less</li> <li>• Single particle composition down to sub-% level</li> <li>• Oxide thickness evaluation with nm- spatial resolution</li> <li>• Composition gradient within single particle</li> </ul>
	XPS	<ul style="list-style-type: none"> <li>• Analytical area: 1.5 mm x 0.6 mm</li> <li>• <math>10^{7-8}</math> particles</li> </ul>	<ul style="list-style-type: none"> <li>• Information depth 10 nm or less</li> <li>• Surface composition above sub-% level</li> <li>• Surface bonding chemistry</li> <li>• Surface contaminants</li> </ul>
	Fractional IGA	<ul style="list-style-type: none"> <li>• 0.1 – 1.0 g</li> <li>• <math>10^6</math> – <math>10^7</math> particles</li> </ul>	<ul style="list-style-type: none"> <li>• O, N and H chemistry speciation (e.g., surface vs bulk) down to ppm level</li> <li>• Quantitation of trace moisture and surface residual -OH polar group down to ppm level</li> </ul>

## REFERENCES

- [1] M. C. Brennan, J. K. Keist and T. A. Palmer, "Defects in Metal Additive Manufacturing," *Journal of Materials Engineering and Performance*, vol. 30, pp. 4808-4818, 2021.
- [2] A. Sola and A. Nouri, "Microstructural porosity in additive manufacturing: The formation and detection of pores in metal parts fabricated by powder bed fusion," *Journal of Advanced Manufacturing and Processing*, vol. 1, no. 3, p. e10021, 2019.
- [3] E. Santecchia, S. Spigarelli and M. Cabibbo, "Material Reuse in Laser Powder Bed Fusion: Side Effects of the Laser—Metal Powder interaction," *Metals*, vol. 10, p. 341, 2020.
- [4] S. Das, "Physical aspects of process control in selective laser sintering of metals," *Adv. Eng. Mater.*, vol. 5, p. 701, 2003.
- [5] I. C. Lippold, *Welding Metallurgy and Weldability*, Hoboken: Wiley, 2015, pp. 1-400.
- [6] J. Hinrichs, "ThermoFisher Scientific Application Note 30142: High purity aluminum analysis," 2019. [Online]. Available: <https://assets.thermofisher.com/TFS-Assets/CMD/Application-Notes/an-30142-gd-ms-high-purity-aluminum-an30142-en.pdf>.
- [7] B. Albouy, J. Berot-Lartigue, N. Cuq and X. Wang, "EAG Application Note: IGA Fractional O N H Analysis of Powder Feedstock for Additive Manufacturing," 2021. [Online]. Available: <https://www.eag.com/resources/brochures/iga-fractional-o-n-h-analyses-of-powder-feedstocks-for-additive-manufacturing/>.
- [8] R. B. David, T. Ohaion-Raz, G. Rafailov and . A. Danon, "Thermal desorption kinetics of H<sub>2</sub>O and H<sub>2</sub> from rapidly solidified Al-Zn-Mg Alloy Powders," *Thermochimica Acta*, vol. 686, p. 178554, 2020.
- [9] C. Weingarten, D. Buchinder, N. Pirch, W. Meiners, K. Wissenbach and R. Poprawe, *J. Mater. Process. Technol.*, vol. 221, p. 112, 2015.
- [10] EAG Laboratories, "EAG Application Note M-050820: Additive Manufacturing (3D Printing): Metallurgical and Materials Services," [Online]. Available: <https://www.eag.com/resources/brochures/additive-manufacturing-3d-printing-metallurgical-and-material-services/>.
- [11] Shcoeck, Libby; Lucak, Kevin; Pompo, Christina; Wang, Xinwei, "White Paper M03195: High Performance Inductively Coupled Plasma – Optical Emission Spectroscopy (HP ICP-OES) for Composition Analysis of Complex Oxides," 2019. [Online]. Available: <https://www.eag.com/resources/whitepapers/high-performance-inductively-coupled-plasma-optical-emission-spectroscopy-hp-icp-oes-for-composition-analysis-of-complex-oxides/>.
- [12] J. Bustillos, J. Kim and A. Moridi, "Exploiting lack of fusion defects for microstructural engineering in additive manufacturing," *Additive Manufacturing*, vol. 48, no. Part A, p. 102399, 2021.
- [13] ASTM F42 / ISOTC261 Committee on Additive Manufacturing Technologies; European Powder Metallurgy Association. *Introduction to Additive Manufacturing Technology*; NISTIR 7873 - *Properties of Metal Powders for Additive Manufacturing: A Review of the State of the Art of Metal Powder Property Testing*.